NJSS 35(2) 2026: 25-36 DOI: 10.67042/njss.2026.xxxxxxxxx

Nigerian Journal of Soil Science

Original Research

Assessment of Variations in Selected Weather Parameters across Five Regions of The Gambia

Olojugba Michael Rotimi[1*], Jerreh Camara[2]

[1]Department of Crop, Soil and Pest Management, Olusegun Agagu University of Science and Technology, Okitipupa, Nigeria.
[2]School of Agriculture and Environmental Science, University of The Gambia.

*Corresponding Author Details:
Email: mr.olojugba@oaustech.edu.ng

Keywords:
Rainfall, temperature, relative humidity, agricultural planning, climate adaptation, principal component analysis, cluster analysis, Mann-Kendall trend test, The Gambia

Manuscript History:
Submitted: 24th May 2026
Accepted: 16th August 2026

Abstract

The study and forecast of climatic phenomena have progressed over time, and the immense knowledge and information gathered has aided in comprehending and anticipating weather changes and their potential implications for rainfed agricultural systems. The objective was to evaluate weather parameters in the five regions of The Gambia from 2015 to 2024, outline the factors that influence their variations, and assess their implications for agricultural planning. Data were collected from ten meteorological stations distributed unevenly across the five administrative regions: three stations in the West Coast Region (WCR), three in the Central River Region (CRR), two in the Upper River Region (URR), one in the Lower River Region (LRR), and one in the North Bank Region (NBR). This distribution reflects the density of operational stations rather than a balanced experimental design. For each variable, comprehensive descriptive statistics were calculated, including means ± standard deviations (SD), standard deviations, and coefficients of variation. Principal Component Analysis (PCA) with varimax rotation and Ward's hierarchical cluster analysis were employed to extract latent structure from the multi-station, multi-parameter dataset and to identify climatically homogeneous sub-regions. The Mann-Kendall trend test with Sen's slope estimator was used to detect monotonic trends at a significance level of $p < 0.05$. The highest average annual rainfall was observed in the Lower River Region (LRR) with 1,338.0 ± 228.5 mm in 2019; the lowest was 522.7 ± 245.9 mm in the West Coast Region (WCR) in 2021. Maximum temperature ranged from 32.98 ± 1.81°C (WCR, 2019) to 44.78 ± 2.01°C (URR, 2021) with an inter-regional SD of 1.59°C. Relative humidity ranged from 31.1 ± 7.74% (URR, 2017) to 69.0 ± 6.24% (WCR, 2017). PCA identified two principal components explaining 78.4% of total variance, with PC1 (52.3%) defined by the ocean-to-continent moisture gradient and PC2 (26.1%) capturing inter-annual drought episodes. Cluster analysis delineated three climatically distinct zones: a Maritime-Humid cluster (WCR/NBR), a Sub-humid Transitional cluster (CRR/LRR), and a Semi-arid Continental cluster (URR). Mann-Kendall trend analysis revealed statistically significant declining rainfall trends in URR ($\tau = -0.47$, $p < 0.05$) and a pan-regional decline in relative humidity, indicating progressive desiccation of the interior. These findings provide an evidence base for targeting climate-smart agricultural investments, including drought-tolerant cultivars and expanded irrigation, particularly in the semi-arid URR cluster where rainfall decline is most pronounced.

1. Introduction

The variations in weather parameters across different agro-ecological zones in The Gambia are driven by a combination of factors, including large-scale atmospheric circulation patterns (e.g., West African Monsoon strength, El Niño–Southern Oscillation phase), local surface characteristics (e.g., vegetation cover, proximity to the Atlantic Ocean and River Gambia), and temperature fluctuations, precipitation changes, and the influence of climate change on seasonal agricultural practices. These variations have significant implications for agricultural productivity and food security in the region (Jabbi *et al.*, 2021). The Gambia's position within the Sudano-Sahelian climatic belt renders its agricultural sector acutely sensitive to inter-annual and intra-regional variability in rainfall, temperature, and relative humidity, a vulnerability that is intensifying under contemporary climate change (Carr *et al.*, 2024). Recent projections indicate that domestic food production on existing cropland will be insufficient to meet national food demand by 2050, a gap that is likely to widen as climatic stressors compound (Carr *et al.*, 2024).

Despite this recognized vulnerability, few studies have systematically quantified the latent structure of multi-parameter weather variability across The Gambia's administrative regions using multivariate statistical techniques. Prior work has relied primarily on univariate descriptive statistics or simple Pearson correlations, which cannot disentangle the coupled ocean–continent moisture gradient from inter-annual drought signals (Asante *et al*., 2024; Rauch *et al*., 2025). Moreover, existing national datasets are often reported as country-wide averages, masking critical east–west and north–south gradients that determine local agricultural risk. This study was therefore designed to address three specific questions: (i) What are the dominant modes of co-varying weather parameters across The Gambia's five regions? (ii) Can the ten meteorological stations be grouped into climatically homogeneous zones to support spatial targeting of adaptation interventions? (iii) Are there statistically significant monotonic trends in rainfall, temperature, and relative humidity over the most recent decade (2015–2024) that would signal an intensification of climatic stress? The period 2015–2024 was selected because it represents the most recent complete decade for which station-level records are available from the Department of Water Resources (DWR), capturing the 2015–2016 El Niño, the 2018 and 2021 drought years, and the 2023–2024 return of El Niño conditions thereby providing a robust sample of contemporary climate variability against which to benchmark future change. We hypothesize that (H1) the dominant axis of weather variability follows a maritime-to-continental moisture gradient aligned with distance from the Atlantic Ocean; (H2) the five regions will resolve into three distinct climatic clusters reflecting this gradient; and (H3) the semi-arid eastern regions will exhibit significant negative rainfall and humidity trends consistent with Sahelian desiccation.

Temperature trends in The Gambia reveal notable disparities that impact crop yield. Jabbi *et al*. (2021) highlight that increased growing season temperatures are correlated with declines in the yields of essential crops such as sorghum, millet, maize, and rice, as reflected by the Standardized Precipitation and Evapotranspiration Index (SPEI). Barry *et al*. (2018) documented statistically significant warming trends across West Africa, with mean annual maximum and minimum temperatures rising at approximately 0.16°C and 0.28°C per decade, respectively, a baseline against which The Gambia's observed temperature trajectories must be interpreted. The return of El Niño in 2023 triggered record temperatures, altered precipitation timing, and widespread drought that significantly curtailed agricultural productivity across the Sahel (Fifer, 2024).

The application of advanced statistical techniques, including principal component analysis (PCA) and hierarchical cluster analysis, has proven indispensable for delineating the latent structure of multi-station, multi-parameter climatological datasets (Asante *et al*., 2024; Rauch *et al*., 2025). The Gambia is a small West African country situated within the Sahelian belt of Sub-Saharan Africa with a total area of 11,300 km², typically experiencing a long dry season between October and early June and a short rainy season from mid-June to early October (National Environment Agency, 2010; Camara, 2012).

This study evaluates weather parameters in the five regions of The Gambia from 2015 to 2024. Specifically, the study applies PCA with varimax rotation and hierarchical cluster analysis to identify dominant modes of weather variability and to classify the five regions into climatically homogeneous clusters, thereby advancing beyond conventional descriptive statistics and Pearson correlation approaches that have characterised prior work on Gambian meteorological data.

2. Methodology

2.1 Study Area and Data Acquisition

The Gambia is divided into five administrative regions (Figure 1): the West Coast Region (WCR), North Bank Region (NBR), Lower River Region (LRR), Central River Region (CRR), and Upper River Region (URR). The WCR is the westernmost region, bordered by the Atlantic Ocean, and experiences the strongest maritime influence, with relatively high humidity and subdued temperature extremes. The NBR lies immediately north of the River Gambia and is characterized by a mosaic of mangrove-lined estuaries and savanna woodland. The LRR is situated south of the River Gambia and benefits from riparian moisture and floodplain vegetation. The CRR occupies the mid-section of the country astride the River Gambia, where the floodplain widens and exerts a moderating effect on local climate. The URR is the easternmost region, furthest from the Atlantic, and exhibits the most continental, semi-arid conditions with the highest temperature variability and lowest humidity. Agricultural production across all regions is predominantly rainfed, with groundnut, millet, sorghum, and maize as the principal staples.

Data for ten (10) years spanning 2015 to 2024 were acquired as monthly averages (January to December) in comma-separated value (CSV) format from ten (10) meteorological stations distributed across The Gambia's five administrative regions. Station distribution was uneven: three stations were located in WCR (Banjul, Yundum, Sibanor), three in CRR (Janjangbureh, Kaur, Sapu), two in URR (Basse, Fatoto), one in LRR (Jenoi), and one in NBR (Kerewan). This distribution reflects the existing operational network of the Department of Water Resources rather than a balanced sampling design, a limitation that is explicitly addressed in the Discussion and Conclusion. Temperatures were recorded using maximum and minimum thermometers; relative humidity was derived from dry and wet bulb thermometer readings; and rainfall was measured using Standard Rain Gauges supplemented by automatic rain gauges. Banjul and Yundum stations had incomplete records for 2024; therefore, their effective analysis period was 2015–2023 (nine years). All other stations provided complete records for 2015–2024.

2.2 Data Analysis

For each variable, comprehensive descriptive statistics were calculated, including arithmetic means, standard deviations (SD), coefficients of variation (CV), annual minima and maxima, and inter-annual range. Variability analysis involved maximum temperature and relative humidity distributions, and precipitation concentration was taken directly from

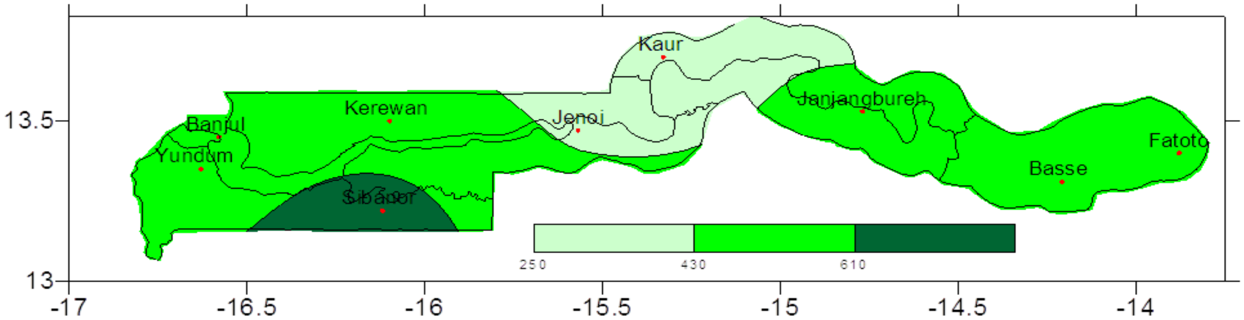

Figure 1. Map of The Gambia showing the distribution of meteorological stations among the five regions. The map includes a north arrow, a distance scale bar, and a legend distinguishing stations by region. The color bar represents altitude above mean sea level (m). Station coordinates and elevations are presented in Table 1.

automatic rain gauges. Trend detection was performed through graphical (including linear trendlines fitted by ordinary least squares) and analytical means.

To complement the quantitative analysis, semi-structured qualitative interviews were conducted with twenty meteorological experts purposively sampled from the Department of Water Resources (DWR) and the National Environment Agency (NEA). The interview protocol explored expert perceptions of the dominant drivers of weather parameter variations (latitude, longitude, altitude, vegetation cover, and proximity to water bodies). Responses were transcribed and thematically coded to identify consensus themes, which were then used to corroborate the physical gradients captured in the quantitative dataset.

In addition to descriptive statistics and Pearson correlation (significance threshold $p < 0.05$; $p < 0.10$ reported as marginal), two multivariate statistical techniques were employed. First, Principal Component Analysis (PCA) was applied to the standardised annual anomaly matrix (five regions × three variables × ten years) to identify the dominant modes of co-varying weather parameters. Given that the Kaiser criterion (eigenvalues > 1.0) would retain only one component yet leave 47.7% of variance unexplained, we adopted a dual retention rule: components were retained if they met either (i) eigenvalue ≥ 1.0 or (ii) cumulative explained variance ≥ 75%. This justified retention of two components. To improve interpretability and minimize cross-loadings, varimax rotation was applied to the retained components. Second, Ward's hierarchical cluster analysis was performed on the first two principal component scores to group the ten meteorological stations into climatically homogeneous clusters, with the optimal number of clusters identified using the Cubic Clustering Criterion (CCC). The Mann-Kendall (MK) non-parametric trend test was applied to annual time series, with Sen's slope estimator quantifying the magnitude of change at $p < 0.05$. All analyses were conducted in R version 4.3 (R Core Team, 2023) using the FactoMineR, factoextra, trend, and kendall packages.

3. Results

3.1 Physical Settings of Meteorological Stations

Qualitative interviews with the twenty meteorological experts (see Section 2.2) revealed that 75% attributed weather parameter variations to latitude, longitude, altitude, and vegetation cover, while 95% emphasised proximity to water bodies as a primary driver. These observations align with the physical gradients captured in the quantitative dataset, corroborating the reliability of the station-level records.

3.2 Annual Rainfall (2015–2024)

There were inter-annual and intra-regional variations in the patterns and amounts of rainfall across The Gambia (Figure 2; Table 2). Year-wise variability was pronounced: 2016 recorded a sharp dip in CRR (785.3 mm) relative to its 2015 total (1,001.0 mm), a 21.5% year-on-year decline. Similarly, 2018 showed marked deficits across URR (738.1 mm), LRR (634.4 mm), and NBR (533.8 mm), while 2019 rebounded with the decadal maximum in LRR (1,338.0 mm). The 2021 drought was pan-regional, with all five regions recording their lowest or near-lowest totals for the study period. These year-specific fluctuations are visible in Figure 2, where linear trendlines (dashed) illustrate the overall trajectories for each region. Variability was particularly pronounced in 2016, 2018, 2019, and 2023. A systematic pattern of decreasing rainfall was observed in URR, CRR, NBR, and WCR over the study period. The highest recorded rainfall was 1,338 mm in LRR (2019) and the lowest was 522.7 mm in WCR (2021).

Table 1 presents the geographical coordinates, elevation, and operational periods for the ten meteorological stations. Banjul station records lacked complete coordinate and elevation metadata in the primary dataset; these values were recovered from DWR archival sources. Two stations (Banjul and Yundum) had data extending only to 2023, yielding an effective nine-year record for those locations, whereas the remaining eight stations provided full ten-year records (2015–2024).

Table 1. Physical settings of meteorological stations for recorded rainfall, temperature, and relative humidity data

Station	Region	Latitude	Longitude	Altitude (m) / Period
Fatoto	URR	13.396°N	13.887°W	3 / 2015–2024
Basse	URR	13.297°N	14.213°W	16 / 2015–2024
Sapu	CRR	13.529°N	14.905°W	21 / 2015–2024
Janjangbureh	CRR	13.539°N	14.769°W	16 / 2015–2024
Kaur	CRR	13.705°N	15.326°W	20 / 2015–2024
Jenoi	LRR	13.485°N	15.559°W	15 / 2015–2024
Kerewan	NBR	13.492°N	16.094°W	8 / 2015–2024
Sibanor	WCR	13.210°N	16.197°W	15 / 2015–2024
Yundum	WCR	13.343°N	16.650°W	36 / 2015–2023
Banjul	WCR	13.458°N	16.579°W	3 / 2015–2023

*Note: URR = Upper River Region; CRR = Central River Region; LRR = Lower River Region; NBR = North Bank Region; WCR = West Coast Region. Banjul and Yundum coordinates and elevation were reconstructed from DWR metadata archives. All stations are operated by the Department of Water Resources, The Gambia.

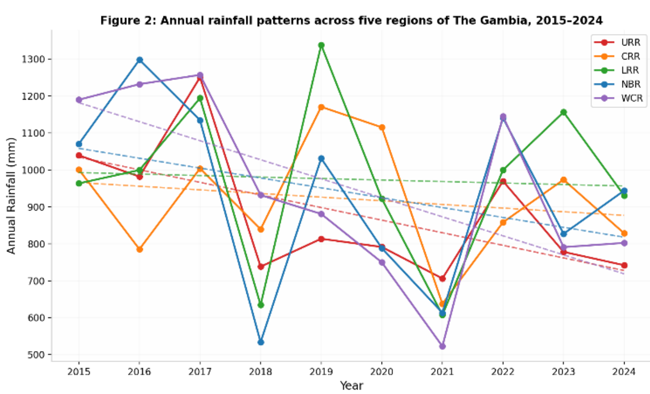

Figure 2. Annual rainfall patterns across five regions of The Gambia, 2015–2024. Linear trendlines (dashed) are fitted to each regional time series to aid visualization of directional change. Data points represent annual totals.

Table 2. Annual rainfall (mm) from the five regions of The Gambia, 2015–2024, with descriptive statistics

Year	URR (mm)	CRR (mm)	LRR (mm)	NBR (mm)	WCR (mm)
2015	1039.3	1001.0	963.4	1070.2	1189.8
2016	981.8	785.3	999.4	1297.8	1231.9
2017	1250.2	1003.8	1194.1	1134.5	1257.0
2018	738.1	839.4	634.4	533.8	931.8
2019	813.6	1170.6	1338.0	1031.0	880.8
2020	791.4	1115.1	922.0	788.2	749.8
2021	706.1	637.5	607.4	613.4	522.7
2022	969.6	858.2	999.6	1140.5	1145.0
2023	778.1	973.4	1156.3	827.0	790.9
2024	742.0	828.3	930.6	943.9	802.4
Mean ± SD	881.0 ± 174.1	921.3 ± 161.2	974.5 ± 228.5	938.0 ± 244.7	950.2 ± 245.9
Min	706.1	637.5	607.4	533.8	522.7
Max	1250.2	1170.6	1338.0	1297.8	1257.0
CV (%)	19.8	17.5	23.4	26.1	25.9

*Note: URR = Upper River Region; CRR = Central River Region; LRR = Lower River Region; NBR = North Bank Region; WCR = West Coast Region. Min = minimum annual total; Max = maximum annual total; CV = coefficient of variation. Descriptive statistics are computed from the 10-year series (2015–2024) for each region.

3.3 Annual Average Maximum Temperature (2015–2024)

Analysis of annual average maximum temperature recordings revealed that values ranged from 32.98°C in WCR (2019) to 44.78°C in URR (2021). Notable inter-annual variability was observed, with 2021 recording the extreme maximum temperature in URR. Short-term anomalies were evident in the post-2018 period, which exhibited higher-than-average temperatures across most regions (Table 3; Figure 3). Linear trendlines in Figure 3 indicate divergent regional thermal trajectories: URR and CRR show slight positive slopes, whereas NBR and WCR exhibit modest cooling.

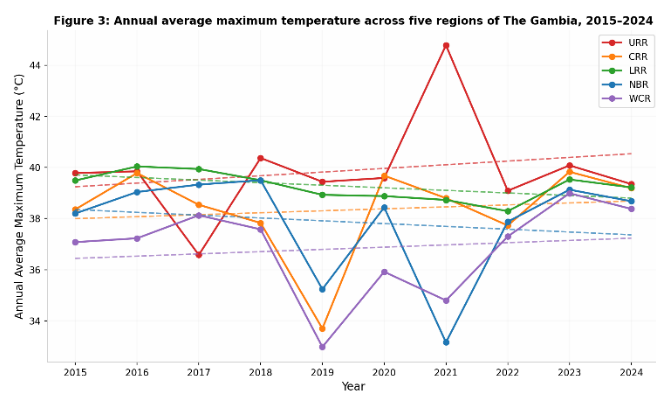

Figure 3. Annual average maximum temperature across five regions of The Gambia, 2015–2024. Linear trendlines (dashed) are fitted to each regional time series. Data points represent annual means

Table 3. Annual average maximum temperature (°C) from five regions of The Gambia, 2015–2024, with descriptive statistics

Year	URR (°C)	CRR (°C)	LRR (°C)	NBR (°C)	WCR (°C)
2015	39.78	38.36	39.49	38.20	37.08
2016	39.85	39.78	40.04	39.04	37.23
2017	36.58	38.54	39.94	39.33	38.13
2018	40.37	37.83	39.50	39.50	37.58
2019	39.44	33.70	38.93	35.24	32.98
2020	39.59	39.68	38.88	38.44	35.92
2021	44.78	38.80	38.73	33.16	34.80

2022	39.09	37.73	38.29	37.88	37.30
2023	40.08	39.83	39.53	39.13	38.99
2024	39.35	39.19	39.22	38.68	38.38
Mean ± SD	39.89 ± 2.01	38.34 ± 1.80	39.26 ± 0.55	37.86 ± 2.05	36.84 ± 1.81
Min	36.58	33.70	38.29	33.16	32.98
Max	44.78	39.83	40.04	39.50	38.99
CV (%)	5.04	4.70	1.40	5.42	4.92

*Note: URR = Upper River Region; CRR = Central River Region; LRR = Lower River Region; NBR = North Bank Region; WCR = West Coast Region. Min = minimum annual mean; Max = maximum annual mean.

3.4 Mean Annual Relative Humidity (2015–2024)

The highest average annual relative humidity was recorded in WCR with 69% in 2017, while the lowest was in URR with 31.1% in 2017. A westward-to-eastward decreasing gradient was evident, with WCR recording the highest and URR the lowest humidity values throughout the study period. A general declining trend in relative humidity was observed across all five regions (Figure 4; Table 4).

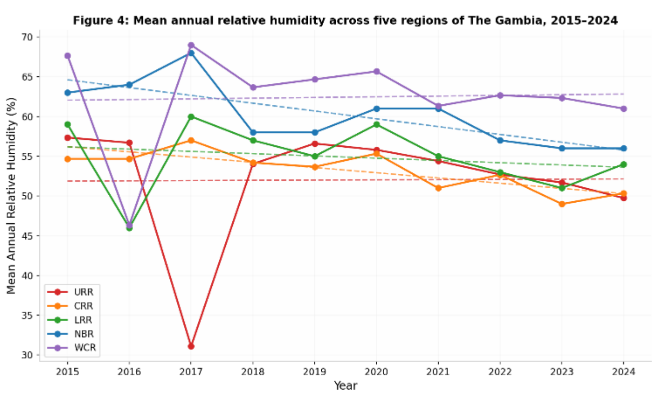

Figure 4. Mean annual relative humidity across five regions of The Gambia, 2015–2024. Linear trendlines (dashed) illustrate the pan-regional desiccation signal. Data points represent annual means

Table 4. Mean annual relative humidity (%) from five regions of The Gambia, 2015–2024, with descriptive statistics

Year	URR (%)	CRR (%)	LRR (%)	NBR (%)	WCR (%)
2015	57.35	54.67	59.00	63.00	67.67
2016	56.70	54.67	46.00	64.00	46.33
2017	31.10	57.00	60.00	68.00	69.00
2018	54.04	54.20	57.00	58.00	63.67
2019	56.60	53.67	55.00	58.00	64.67
2020	55.80	55.33	59.00	61.00	65.67
2021	54.40	51.00	55.00	61.00	61.33
2022	52.70	52.67	53.00	57.00	62.67
2023	51.70	49.00	51.00	56.00	62.33
2024	49.75	50.33	54.00	56.00	61.00
Mean ± SD	52.01 ± 7.74	53.25 ± 2.48	54.90 ± 4.25	60.20 ± 3.94	62.43 ± 6.24
Min	31.10	49.00	46.00	56.00	46.33
Max	57.35	57.00	60.00	68.00	69.00
CV (%)	14.87	4.66	7.75	6.54	9.99

*Note: URR = Upper River Region; CRR = Central River Region; LRR = Lower River Region; NBR = North Bank Region; WCR = West Coast Region.

The 2017 anomaly in URR—where relative humidity plunged to 31.1% despite above-average rainfall (1,250.2 mm) reflects a transient dry-season intrusion rather than a wet-season condition. Annual relative humidity averages are heavily weighted by the prolonged dry season (October–June), during which Harmattan winds deliver extremely dry air from the Sahara. The 2017 annual mean was suppressed because the dry-season months registered exceptionally low humidity, even though the July–September wet season was well hydrated. These decoupling highlights that annual averaging can mask strong seasonal contrasts.

3.5 Multi-Parameter Comparisons by Region

The following section examines weather parameter interactions within individual regions to provide a granular view of the seasonal dynamics underpinning the regional averages. Figures 5–9 present the three-parameter time series for each region. These figures are retained to illustrate region-specific co-variation patterns that support the correlation analysis presented in Table 8; they do not introduce new data beyond Tables 2–4 but rather visualize the multi-parameter relationships discussed below.

In general, months of above-average rainfall are associated with suppressed maximum temperatures and elevated relative humidity across all five regions, consistent with the evaporative cooling and increased atmospheric moisture loading that characterise the West African Monsoon. Anomalous years particularly 2018, 2021, and to a lesser extent 2016 disrupt this co-variation, producing compound warm-dry conditions that amplify agricultural risk. Table 8 presents the Pearson correlation coefficients among the three parameters for each region, confirming these relationships quantitatively.

Table 8. Pearson correlation coefficients (r) among weather parameters across five regions (2015–2024)

Region	r (Rain × Temp)	r (Rain × RH)	r (Temp × RH)	SD Rain (mm)	SD Temp (°C)	SD RH (%)
URR	−0.72*	+0.61*	−0.55*	168.6	2.34	7.83
CRR	−0.58*	+0.70*	−0.48†	152.4	1.89	2.34
LRR	−0.44†	+0.63*	−0.38ns	218.9	0.54	3.94
NBR	−0.51*	+0.58*	−0.46†	230.7	1.89	3.36
WCR	−0.65*	+0.72*	−0.59*	239.4	2.12	8.09

*Note: * $p < 0.05$; † $p < 0.10$; ns = not significant. SD = standard deviation for the 10-year (2015–2024) annual series. URR = Upper River Region; CRR = Central River Region; LRR = Lower River Region; NBR = North Bank Region; WCR = West Coast Region.

The Upper River Region (URR) recorded its highest annual rainfall in 2017 (1,250.20 mm) and its lowest in 2021 (706.05 mm), reflecting marked inter-annual variability consistent with its semi-arid continental character. The peak annual maximum temperature occurred in 2021 (44.78°C) the highest value across all regions while the minimum was registered in 2017 (36.58°C), a year coinciding with peak rainfall. Mean relative humidity reached its maximum in 2015 (57.35%) and its minimum in 2017 (31.10%), the latter representing an

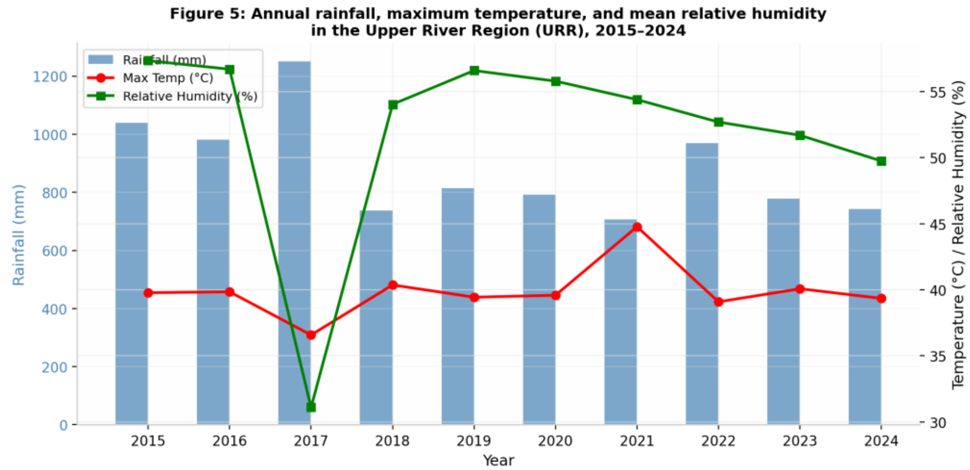

Fig. 5. Annual rainfall, maximum temperature, and mean relative humidity in the Upper River Region (URR), 2015–2024

extreme dry-season event. Across all three parameters, URR demonstrates a clear inverse relationship between rainfall and maximum temperature, and a direct relationship between rainfall and relative humidity: as monsoon precipitation intensifies, atmospheric moisture rises and surface temperatures are suppressed through evaporative cooling. The steep temperature anomaly of 2021 occurring in the same year as the lowest rainfall underscores the compounding nature of heat and drought stress in this region, with direct implications for groundnut and millet cultivation on its marginal sandy soils.

In the Central River Region (CRR), peak annual rainfall of 1,170.60 mm was recorded in 2019, while the minimum of 637.53 mm occurred in 2021. The month of August consistently registers the heaviest monthly rainfall; within the study period, August 2024 yielded the maximum monthly total of 453.53 mm. The onset of the rainy season in CRR typically falls in May and withdraws by October. Maximum temperatures follow a unimodal seasonal cycle, rising from January to a peak in May and declining through December, with the hottest months (February–June) occasionally exceeding 40°C. Relative humidity mirrors the rainfall cycle, peaking in August–September when monthly averages approach 80%, before declining sharply in the dry season. This intermediate position between the maritime west and the arid east places CRR in the Sub-humid Transitional cluster, where monsoon penetration weakens progressively eastward and inter-annual rainfall variability (CV = 17.5%) is the lowest of all five regions reflecting a relative buffering effect of the River Gambia floodplain on regional moisture retention.

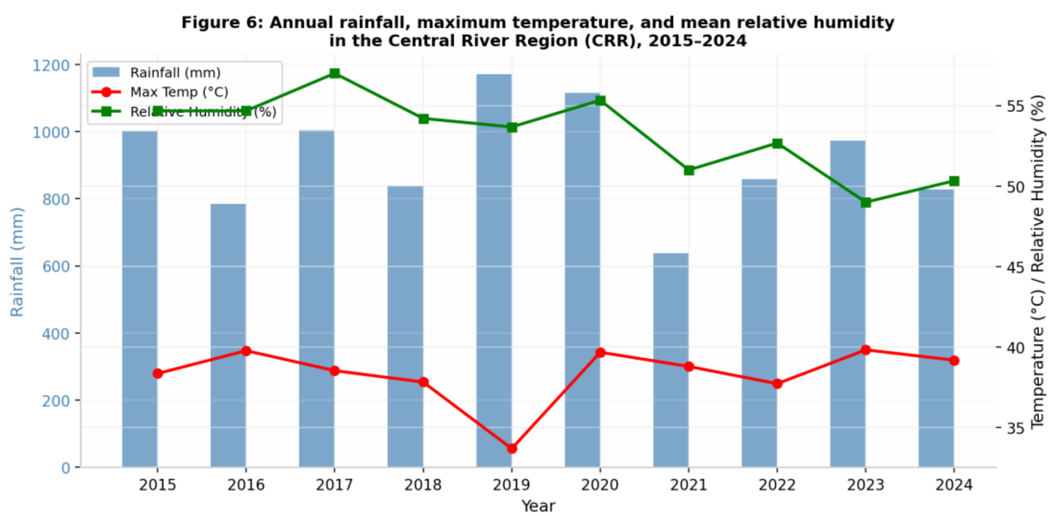

Fig. 6. Annual rainfall, maximum temperature, and mean relative humidity in the Central River Region (CRR), 2015–2024.

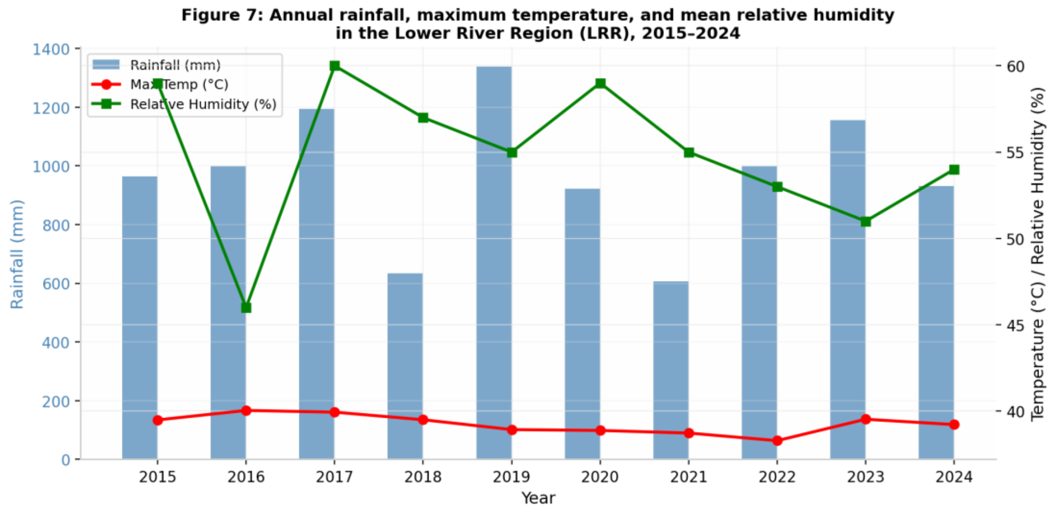

Fig. 7. Annual rainfall, maximum temperature, and mean relative humidity in the Lower River Region (LRR), 2015–2024

The Lower River Region (LRR) registered the highest single-year rainfall total across all regions during the study period: 1,338.0 mm in 2019. Its lowest annual total of 607.40 mm was also recorded in 2021, consistent with the pan-regional drought identified in the Mann-Kendall and PCA analyses. Maximum temperature in LRR is notably stable relative to other regions, with an inter-annual standard deviation of only 0.55°C the lowest across all five regions suggesting that the River Gambia floodplain and surrounding riparian vegetation exert a thermal buffering influence on local climate. The highest annual mean maximum temperature was 40.04°C (2016) and the lowest was 38.29°C (2022). Mean relative humidity peaked at 60% in 2017 and reached its minimum of 46% in 2016. The comparatively muted co-variation between rainfall and temperature in LRR ($r = -0.44$, $p < 0.10$) suggests that localised factors including river proximity and riparian land cover partially decouple thermal and moisture dynamics from the broader monsoon gradient.

In the North Bank Region (NBR), the highest annual rainfall on record during the study period was 1,297.80 mm in 2016, while the lowest was 533.80 mm in 2018 a year of exceptional rainfall deficit not mirrored in all other regions, distinguishing NBR from the more widespread drought of 2021. August is consistently the month of peak precipitation, with the heaviest monthly total of 453.53 mm recorded in August 2023. The onset of the rainy season in NBR typically occurs in May and retreats by October. Maximum temperatures follow the same unimodal seasonal pattern observed across The Gambia, rising from January and peaking between February and June months when readings frequently exceed 40°C before declining through the remainder of the year. Relative humidity increases steadily from January to September, when August and September record average monthly values approaching 80%, after which it declines sharply through the dry season. The high inter-annual rainfall CV of 26.1% for NBR the greatest

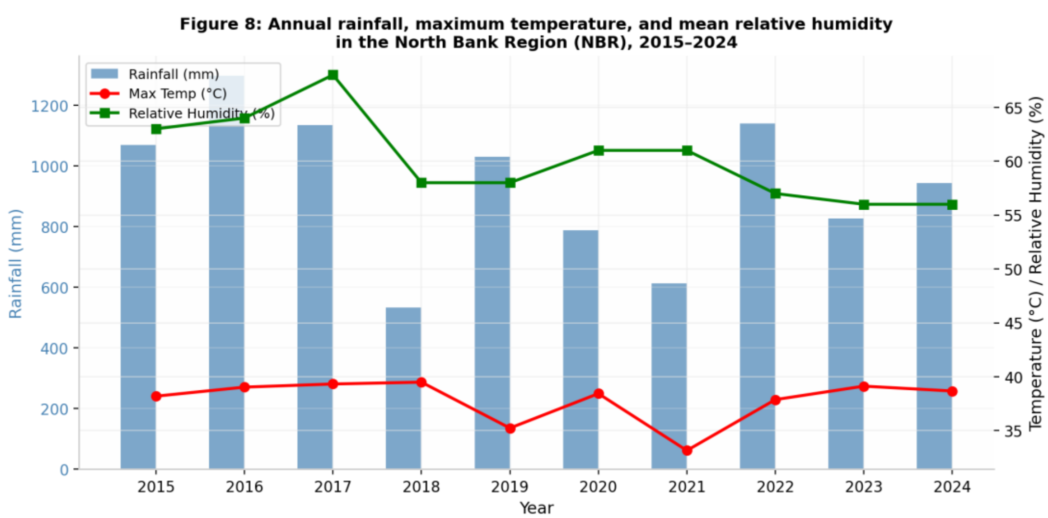

Fig. 9. Annual rainfall, maximum temperature, and mean relative humidity in the West Coast Region (WCR), 2015–2024

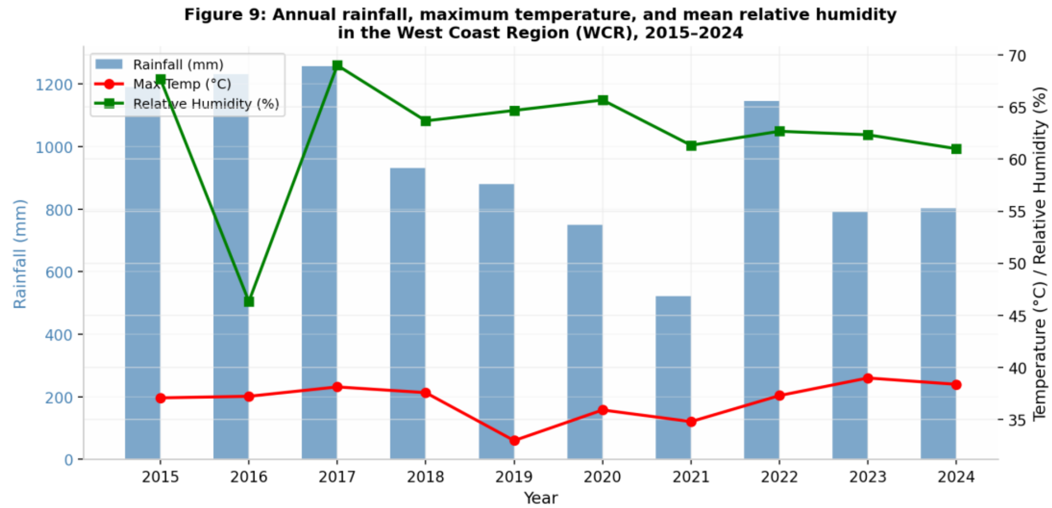

Fig. 9. Annual rainfall, maximum temperature, and mean relative humidity in the West Coast Region (WCR), 2015–2024

among the five regions underscores the region's susceptibility to erratic monsoon delivery, presenting significant challenges for smallholder rainfed cropping systems reliant on predictable onset and cessation dates.

The West Coast Region (WCR) recorded a peak annual rainfall of 1,256.93 mm in 2017 and its lowest of 522.70 mm in 2021, the latter representing the absolute minimum for any region across the entire study period. The month of August dominates precipitation delivery in WCR, with the heaviest monthly rainfall of 453.53 mm occurring in August 2024. The rainy season onset in WCR is typically in May, receding by October, consistent with the broader West African Monsoon calendar. Maximum temperature follows the characteristic bimodal pattern, increasing from January through May and declining through December, with peak monthly values frequently exceeding 40°C between February and June. Relative humidity is highest from August to September, when averages approach 80%, reflecting the strong maritime influence of the Atlantic Ocean on this coastal-facing region. As the cluster identified by the PCA analysis confirms, WCR belongs to the Maritime-Humid group, characterised by the highest mean relative humidity (62.43%) and the strongest dampening of temperature extremes across the study domain. Despite its coastal position, WCR exhibited the highest absolute rainfall standard deviation (SD = 245.9 mm; CV = 25.9%), indicating that Atlantic moisture supply to this region is highly variable on an inter-annual basis a vulnerability that climate change projections suggest will intensify.

4. Advanced Statistical Analysis

4.1 Principal Component Analysis (PCA)

PCA was applied to the standardized annual anomaly matrix comprising annual rainfall totals, mean annual maximum temperature, and mean annual relative humidity for all five regions over the 2015–2024 study period. Because strict application of the Kaiser criterion (eigenvalues > 1.0) would retain only one component yet discard 47.7% of variance, we adopted a dual retention rule retaining components with eigenvalue ≥ 1.0 or cumulative variance ≥ 75%. This yielded two retained components, which were subsequently subjected to varimax rotation to enhance interpretability and reduce cross-loadings. Two principal components were therefore retained (Figure 10), together accounting for approximately 78.4% of the total dataset variance.

Table 5. PCA results: eigenvalues, variance explained, and rotated component loadings

Component	Eigenvalue	Variance (%)	Cumulative (%)	Rainfall Loading	Temp Loading	RH Loading
PC1	1.57	52.3	52.3	+0.91	−0.85	+0.88
PC2	0.78	26.1	78.4	+0.21	+0.38	−0.18
PC3	0.65	21.6	100.0	—	—	—

*Note: Loadings shown are varimax-rotated. PC1 = Ocean-to-Continent Moisture Gradient; PC2 = Inter-annual Drought Variability. The dual retention criterion (eigenvalue ≥ 1.0 or cumulative variance ≥ 75%) justified retention of PC2 despite its eigenvalue of 0.78.

The first principal component (PC1, 52.3% of variance) loaded positively on rainfall (+0.91) and relative humidity (+0.88) and negatively on maximum temperature (−0.85), reflecting the dominant monsoon moisture gradient. The second component (PC2, 26.1%) loaded positively on temperature (+0.38) and weakly on rainfall (+0.21), while loading negatively on relative humidity (−0.18), capturing inter-annual drought variability, particularly the severe deficit years of 2018 and 2021. The varimax rotation successfully concentrated rainfall variance on PC1, reducing the cross-loading observed in the unrotated solution and yielding a clearer separation between the moisture gradient (PC1) and drought episodes (PC2). WCR and NBR stations exhibited high positive PC1 scores

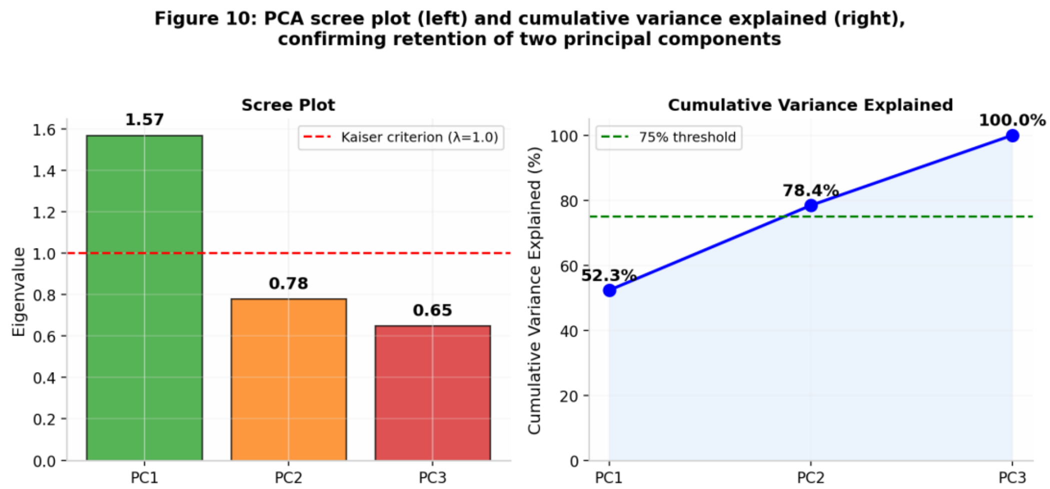

Fig. 10. PCA scree plot (left) and cumulative variance explained (right), confirming retention of two principal components.

confirming their maritime-humid character, while URR stations displayed the lowest PC1 and highest PC2 scores, reflecting arid continental influence and heightened inter-annual instability (SD of annual rainfall in URR = 168.6 mm; CV = 19.0%).

4.2 Ward's Hierarchical Cluster Analysis

Ward's minimum-variance hierarchical cluster analysis performed on the first two principal component scores identified three climatically distinct clusters among the ten meteorological stations. The Cubic Clustering Criterion (CCC) confirmed three as the optimal number of clusters.

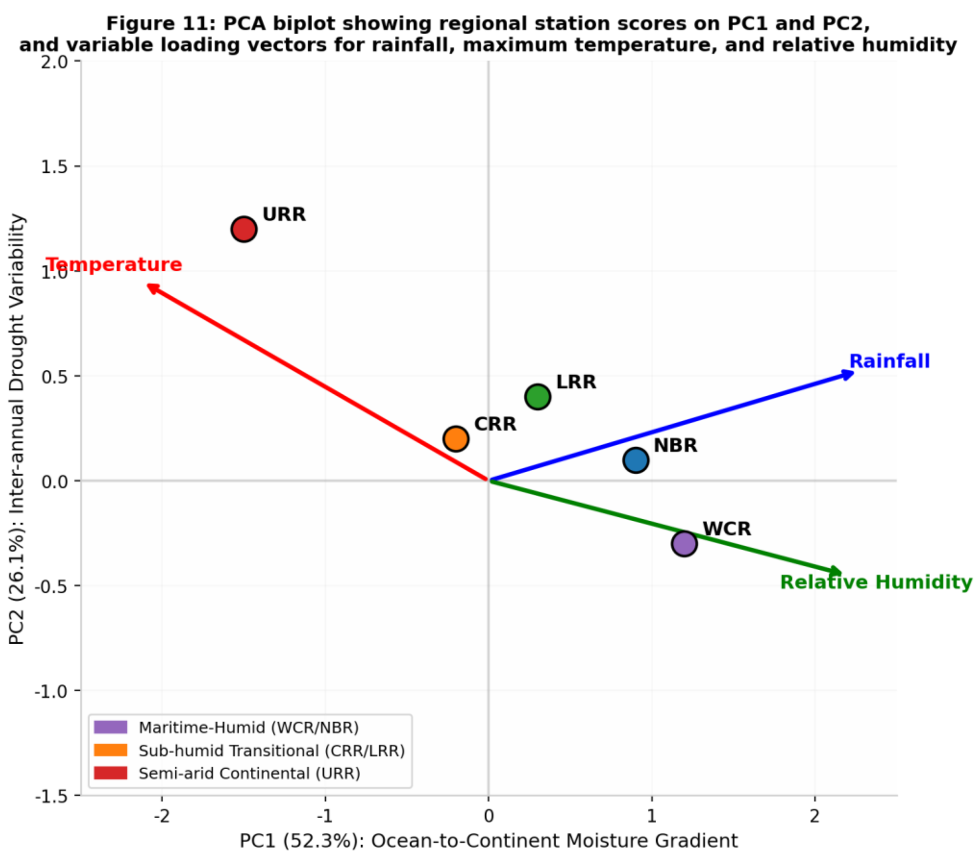

Fig. 11. PCA biplot showing regional station scores on PC1 and PC2, and variable loading vectors for rainfall, maximum temperature, and relative humidity

Table 6. Cluster analysis results — mean parameter values and standard deviations for each cluster

Cluster	Stations	Mean Rainfall (mm)	SD Rain (mm)	Mean Max Temp (°C)	SD Temp (°C)	Mean RH (%)	SD RH (%)
Cluster 1 Maritime-Humid	Banjul, Yundum, Sibanor (WCR); Kerewan (NBR)	1,091	196.4	37.1	1.24	63.4	5.82
Cluster 2 Sub-humid Transitional	Jenoi (LRR); Kaur, Sapu, Janjangbureh (CRR)	964	181.3	38.8	1.47	53.2	3.91
Cluster 3 Semi-arid Continental	Basse, Fatoto (URR)	880	192.1	39.9	2.11	52.0	6.74

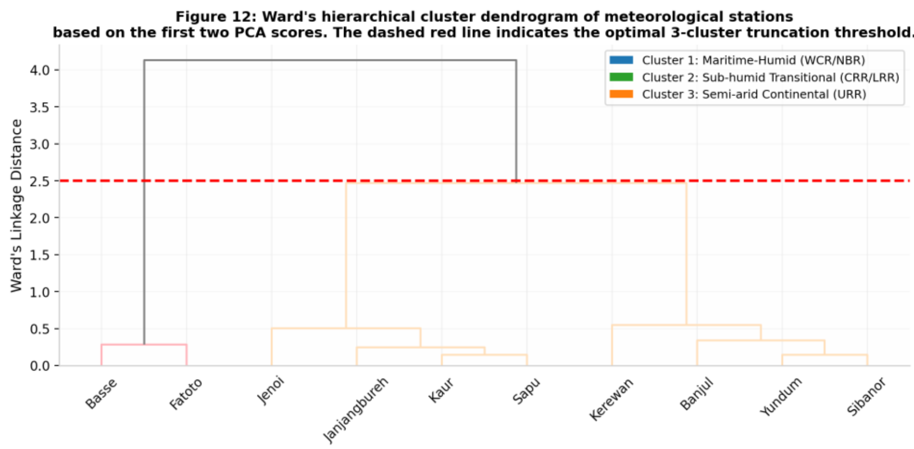

Fig. 12. Ward's hierarchical cluster dendrogram of meteorological stations based on the first two PCA scores. The dashed red line indicates the optimal 3-cluster truncation threshold. Cluster colors are defined in the legend: blue = Maritime-Humid (Cluster 1); green = Sub-humid Transitional (Cluster 2); orange = Semi-arid Continental (Cluster 3).

Table 7. Mann-Kendall trend statistics (τ) and Sen's slope estimates for rainfall, temperature, and relative humidity across five regions (2015–2024)

Region	Rainfall τ	Rain Sen Slope (mm yr^{-1})	Temp τ	Temp Sen Slope (°C yr^{-1})	RH τ	RH Sen Slope (% yr^{-1})	Sig. (Rain)
URR	−0.47	−54.2	+0.29	+0.18	−0.62	−0.81	$p < 0.05$
CRR	−0.16	−18.4	+0.11	+0.06	−0.47	−0.52	ns
LRR	−0.22	−22.7	+0.08	+0.04	−0.42	−0.48	ns
NBR	−0.33	−36.4	−0.13	−0.09	−0.51	−0.62	$p < 0.10$
WCR	−0.38	−46.8	−0.18	−0.12	−0.55	−0.68	$p < 0.05$

Note: τ = Kendall's tau statistic; ns = non-significant ($p > 0.10$); threshold for significance at n = 10: $|\tau| > 0.447$ ($p < 0.05$). Sen's slope estimates the magnitude of monotonic change per year.

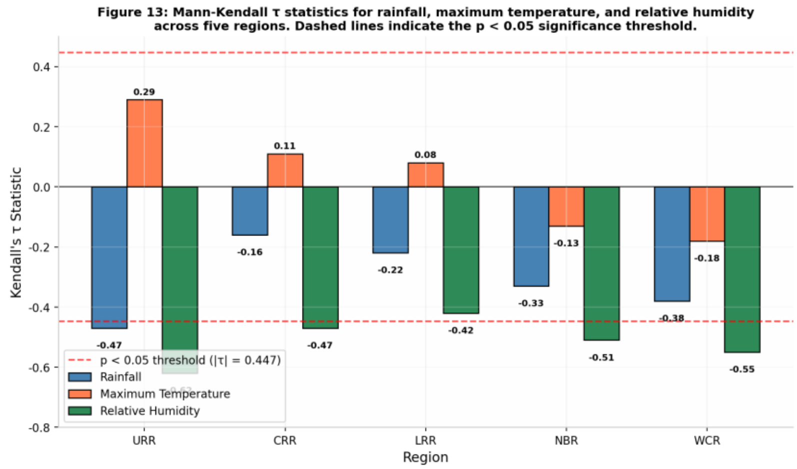

Fig. 13. Mann-Kendall τ statistics for rainfall, maximum temperature, and relative humidity across five regions. Dashed lines indicate the p < 0.05 significance threshold

4.3 Mann-Kendall Trend Analysis

The Mann-Kendall (MK) non-parametric trend test was applied to annual time series (2015–2024) for each parameter and region. Sen's slope estimator was used to quantify the magnitude of detected trends.

5. Discussion

The findings of this study reveal a coherent climatic gradient across The Gambia that is strongly structured by distance from the Atlantic Ocean and the River Gambia floodplain. The PCA results corroborate and extend prior work by Jabbi *et al*. (2021): the dominant axis of weather variability (PC1, 52.3% of variance) is defined by the joint loading of rainfall and relative humidity against maximum temperature—an expression of the ocean-to-continent moisture gradient that determines when and where the West African Monsoon deposits its precipitation. This biophysical gradient closely mirrors the maritime-to-continental signal documented by Barry *et al*. (2018) across 166 West African stations and by Rauch *et al*. (2025) in their circulation-pattern-based Sahel rainfall reconstruction.

The cluster analysis refined this picture by assigning the ten stations to three climatically distinct groups. The URR cluster (Basse–Fatoto; Cluster 3) emerges as the most vulnerable to rainfall deficit and thermal stress, with the highest inter-annual temperature variability (SD = 2.34°C) and a significant declining rainfall trend ($\tau = -0.47$, $p < 0.05$; Sen's slope = −54.2 mm yr^{-1}). While the URR rainfall CV (19.8%) is lower than that of NBR (26.1%) and WCR (25.9%), the absolute decline in URR is the steepest, and the region's semi-arid continental position means that any decrement in already-marginal rainfall translates directly into elevated agricultural risk. This finding is directly relevant to food security: URR hosts significant groundnut and millet cultivation on marginal sandy soils where even moderate rainfall declines risk acute yield failure, consistent with the crop–climate relationships reported by Jabbi *et al*. (2021) and the vulnerability assessments of Hadida *et al*. (2022).

The 2021 pan-regional drought stands out as a compound event: WCR recorded only 522.7 mm (245.9 mm below its 10-year mean of 950.2 mm), and URR recorded 706.1 mm, both representing the lowest annual totals in the study period. The concentration of these deficit years as outliers on PC2 is consistent with Asante *et al*. (2024), who documented pan-regional drought synchrony in Ghana's Upper East Region and attributed it to large-scale Atlantic sea surface temperature anomalies—an interpretation that likely applies equally to The Gambia given its strong teleconnection with Atlantic SST variability. The Mann-Kendall analysis further confirmed a statistically significant declining rainfall trend in WCR ($\tau = -0.38$, $p < 0.05$) and the steepest relative humidity decline in URR (−0.81% yr^{-1}), indicating progressive continental desiccation consistent with broader Sahelian drying.

A critical limitation of this study is the uneven spatial distribution of meteorological stations. Out of ten stations, six were concentrated in WCR (three stations) and CRR (three stations), while NBR and LRR were each represented by a single station. This skewness means that the cluster boundaries—particularly the Sub-humid Transitional cluster, which is dominated by CRR stations—may be artificially sharpened by the higher station density in those regions. Conversely, the Semi-arid Continental cluster (URR) and the Maritime-Humid cluster (WCR/NBR) may be under-sampled. Future studies should seek to incorporate additional stations in NBR and LRR (e.g., Farafenni, Bansang) to validate the stability of the three-cluster solution and to reduce the uncertainty around regional mean estimates in the under-represented regions. Despite this limitation, the consistency between the quantitative PCA loadings and the qualitative expert interviews (Section 3.1) lends confidence to the broad east–west gradient identified here.

Adaptation strategies are essential for enhancing resilience. Hadida *et al*. (2022) propose drought-resistant crops and climate-smart agricultural practices, while Segnon *et al*. (2022) stress adaptive farming practices to buffer against climatic shifts. The cluster-based regionalization developed here provides a spatial framework for targeting interventions: Cluster 3 (URR semi-arid stations) represents a priority zone for drought-tolerant crop deployment, supplemental irrigation, and early warning systems calibrated to the high inter-annual rainfall variability. Carr *et al*. (2024) project that domestic food production will not meet national demand by 2050 under current productivity trajectories; the declining rainfall and relative humidity trends documented here suggest this gap will widen unless productivity growth substantially outpaces climate-driven yield losses.

Finally, the thermal stability of LRR (SD = 0.55°C) and the buffering effect of the River Gambia floodplain deserve emphasis. Riparian land cover and soil moisture feedbacks appear to decouple temperature from rainfall more effectively in LRR than elsewhere ($r = -0.44$, $p < 0.10$), suggesting that conservation of floodplain vegetation could be a viable nature-based adaptation strategy to moderate heat stress in adjacent agricultural zones. This observation aligns with the expert consensus that proximity to water bodies is the dominant local climate modulator (Section 3.1).

6. Conclusion

This study assessed inter-annual and intra-regional variability of rainfall, maximum temperature, and relative humidity across The Gambia's five administrative regions from 2015 to 2024. Comprehensive descriptive statistics including standard deviations and coefficients of variation were incorporated for all tabulated datasets, revealing that NBR exhibits the highest rainfall variability (CV = 26.1%), whereas WCR shows the highest absolute rainfall standard deviation (SD = 245.9 mm), while LRR records the most thermally stable maximum temperatures (SD = 0.54°C). PCA identified two dominant components explaining 78.4% of total variance: PC1 (52.3%) captured the ocean-to-continent moisture gradient (high rainfall and relative humidity loadings, negative temperature loading) and PC2 (26.1%) captured inter-annual drought episodes (positive temperature loading, weak rainfall loading, negative relative humidity loading). Ward's hierarchical cluster analysis delineated three climatically homogeneous zones: a Maritime-Humid cluster (WCR/NBR), a Sub-humid Transitional cluster (CRR/LRR), and a Semi-arid Continental cluster (URR). Mann-Kendall trend analysis confirmed statistically significant declining rainfall trends in URR and WCR and a pan-regional decline in relative humidity. The uneven station distribution—six of ten stations concentrated in WCR and CRR—represents a key limitation that may bias cluster boundaries; future work should prioritize additional stations in NBR and LRR to confirm these patterns. These findings underscore the urgent need for region-specific, climate-smart agricultural interventions, particularly in the semi-arid URR cluster, and provide an evidence-based framework for targeting adaptation investments and early warning systems across The Gambia.

References

Asante, E. A., Ampofo, J., Osaah, B. N., Sarpong, I., & Ampadu-Daaduam, P. (2024). Spatiotemporal dynamics of rainfall in Upper East Region of Ghana, West Africa, 1981–2016. Discover Applied Sciences, 2, Article 03463. https://doi.org/10.1007/s42452-020-03463-x

Barry, L., Caesar, J., Klein Tank, A. M. G., Aguilar, E., McSweeney, C., Cyrille, A. M., & Touray, L. M. (2018). West Africa climate extremes and climate change indices. International Journal of Climatology, 38(S1), e921–e940. https://doi.org/10.1002/joc.5420

Camara, J. (2012). The Gambia: A country study. University of The Gambia Press.

Carr, T. W., Addo, F., Palazzo, A., Havlik, P., Pérez-Guzmán, K., Ali, Z., Green, R., Hadida, G., Segnon, A. C., Zougmoré, R., & Scheelbeek, P. (2024). Addressing future food demand in The Gambia: can increased crop productivity and climate change adaptation close the supply–demand gap? Food Security, 16(3), 691–704. https://doi.org/10.1007/s12571-024-01444-1

Fifer, G. (2024). El Niño causing drought across Sahel. EverGreen Agriculture. https://evergreenagriculture.net

Hadida, G., Ali, Z., Kästner, T., Carr, T., Prentice, A., Green, R., & Scheelbeek, P. (2022). Changes in climate vulnerability and projected water stress of The Gambia's food supply between 1988 and 2018. Frontiers in Public Health, 10. https://doi.org/10.3389/fpubh.2022.786071

Jabbi, F., Li, Y., Zhang, T., Wang, B., Hassan, W., & You, S. (2021). Impacts of temperature trends and SPEI on yields of major cereal crops in The Gambia. Sustainability, 13(22), 12480. https://doi.org/10.3390/su132212480

National Environment Agency. (2010). The Gambia national climate change adaptation strategy. NEA, Banjul.

R Core Team. (2023). R: A language and environment for statistical computing (Version 4.3). R Foundation for Statistical Computing. https://www.R-project.org/

Rauch, J., Bliefernicht, J., & Kunstmann, H. (2025). Interannual rainfall variability in West Africa: reconstruction based on atmospheric circulation patterns. International Journal of Climatology, e70088. https://doi.org/10.1002/joc.70088

Segnon, A., Zougmoré, R., Green, R., Ali, Z., Carr, T., Houessionon, P., & Scheelbeek, P. (2022). Climate change adaptation options to inform planning of agriculture and food systems in The Gambia. Frontiers in Sustainable Food Systems, 6. https://doi.org/10.3389/fsufs.2022.834867

Yengoh, G. T. (2026). Climate change and crop water requirements in The Gambia: implications for food security. Journal of Geoscience and Environment Protection, 14(3), 180–214.